

1 **Evolution to increased positive charge on the viral spike protein may be part of**  
2 **the adaptation of SARS-CoV-2 to human transmission.**

3  
4 **Matthew Cotten\***, My V.T. Phan

5  
6 Author affiliations: Medical Research Council–University of Glasgow Centre for Virus  
7 Research, Glasgow, Scotland, UK (MC), UK Medical Research Council–Uganda  
8 Virus Research Institute and London School of Hygiene and Tropical Medicine  
9 Uganda Research Unit, Entebbe, Uganda (MC, MVTP); UK

10  
11 \*Correspondence to Matthew Cotten, email: [matthew.cotten@lshtm.ac.uk](mailto:matthew.cotten@lshtm.ac.uk)

12  
13 **Abstract**

14 The severe acute respiratory syndrome coronavirus 2 ( SARS-CoV-2), the causative agent of  
15 the coronavirus disease 2019 (COVID-19) pandemic, continues to evolve and infect individuals. The  
16 exterior surface of the SARS-CoV-2 virion is dominated by the spike protein and the current work  
17 examined spike protein biochemical features that have changed during the 2 years that SARS-CoV-2  
18 has infected humans. These biochemical properties may influence virion survival and promote  
19 movement through the environment and within the human airway to reach target cells to bind, enter  
20 and establish the next round of infection. In addition to selective pressure to avoid immune  
21 recognition of viral proteins, we hypothesised that SARS-CoV-2 emerged from an animal reservoir  
22 capable of human infection and transmission but in a sub-optimum state and a second level of  
23 selective pressure is acting on these biochemical features. Our analysis identified a striking change in  
24 spike protein charge, from -8.3 in the original Lineage A and B viruses to -1.26 in the current Omicron  
25 viruses. In summary, we conclude that in addition to immune selection pressure, the evolution of  
26 SARS-CoV-2 has also altered viral spike protein biochemical properties. Future vaccine and  
27 therapeutic development should also exploit and target these biochemical properties.

28  
29 **Introduction**

30 The severe acute respiratory syndrome coronavirus 2 ( SARS-CoV-2), the causative agent of  
31 the coronavirus disease 2019 (COVID-19) epidemic, continues to evolve and infect individuals.  
32 Similar to other viruses, the SARS-CoV-2 virion biochemical properties play an important role in  
33 controlling virus transmission. After replication in an infected individual and release from an infected  
34 cell, onward transmission requires survival of the virion to reach susceptible cells in a new host  
35 individual initiating the next round of infection. The physical properties of the surface proteins of the  
36 virus such as charge, size, hydrophobicity and folding may influence movement of the virion through

37 the environment, promoting or limiting binding of the virion to the external surfaces. Once reaching a  
38 susceptible individual, virion physical properties may influence movement within the human airway  
39 and determine the ability of an infecting virion to reach target cells to bind, enter and replicate  
40 (Adamczyk et al. 2021). The exterior surface of the SARS-CoV-2 virion is dominated by the spike  
41 protein and the current work examines simple spike protein features that have changed during the 2  
42 years of the SARS-CoV-2 pandemic. In addition to selective pressure to avoid immune recognition of  
43 viral proteins, we hypothesise that SARS-CoV-2 emerged from an animal reservoir capable of human  
44 infection and transmission but in a sub-optimum state. Additionally, there is a second level of  
45 selective pressure to adjust to the physical transmission between humans. Evidence for this  
46 adaptation can be found in changes in the SARS-CoV-2 spike protein over recent evolution. With over  
47 11 million SARS-CoV-2 genomic sequences generated globally from across the pandemic, many of  
48 these sequences have intact spike gene sequences that can be used to monitor change across the 2  
49 years of human host evolution of this virus.

50 Much of the observed spike protein substitutions may be in response to the developing  
51 immune response to this new pathogen, which is reflected in substitutions occurring in the immune-  
52 exposed S1 domain of the spike protein and there is ample evidence that many of these spike protein  
53 changes allow escape from host immunity (Tzou et al. 2022)(Greaney, Loes, et al. 2021)(Greaney,  
54 Starr, et al. 2021)(Greaney et al. 2022) (Cao et al. 2022) (Dejnirattisai et al. 2022) (DeGrace et al.  
55 2022). There may also be evolutionary selection for protein changes that improve host interactions  
56 apart from immune evasion. These include altering spike/receptor binding kinetics, protease cleavage  
57 events, tertiary structure (S1/S2 interactions after cleavage) or the physical properties of the virion  
58 (charge, hydrophobicity, and protein folding or secondary structure) in ways that might improve  
59 transmission. To explore the role of the biochemical features of the spike protein in human  
60 transmission, we monitored changes in spike biochemical features over the two years that SARS-  
61 CoV-2 has been evolving in humans and report an increase in spike protein positively charge  
62 especially among the virus lineages that were highly prevalent.

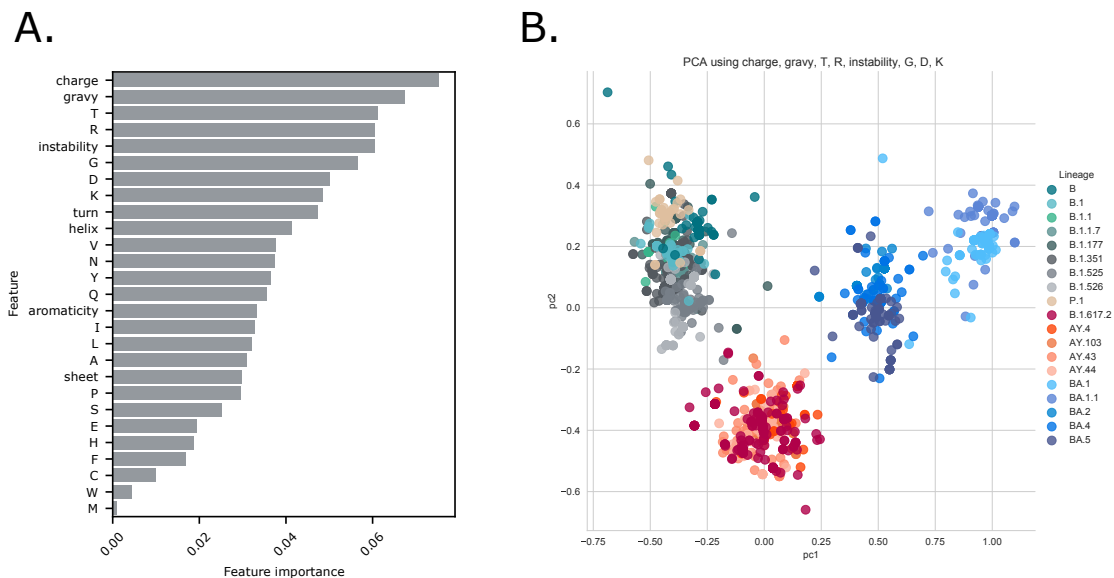
63

## 64 **Results.**

65 The SARS-CoV-2 spike protein physical features were calculated from spike protein  
66 sequences from across 2 years of the COVID-19 epidemic. Features that could be quantitated from  
67 protein sequence were used (see Methods), including charge at pH 7.4, Kyle and Doolittle GRAVY  
68 score (Kyte & Doolittle 1982) (which is a measure of hydrophobicity), an instability index derived from  
69 dipeptide content (Guruprasad et al. 1990), properties influencing protein folding (percent helix, fold or  
70 sheet as predicted from amino acid content), individual amino acid total fraction and di-amino acid  
71 total fraction.

72 A dominant pattern of SARS-CoV-2 evolution during the two years of human adaptation has  
73 been the regular appearance and the subsequent regional and then global dominance of lineages.  
74 These lineages typically encode a small set of amino acid changes from earlier lineages, many of

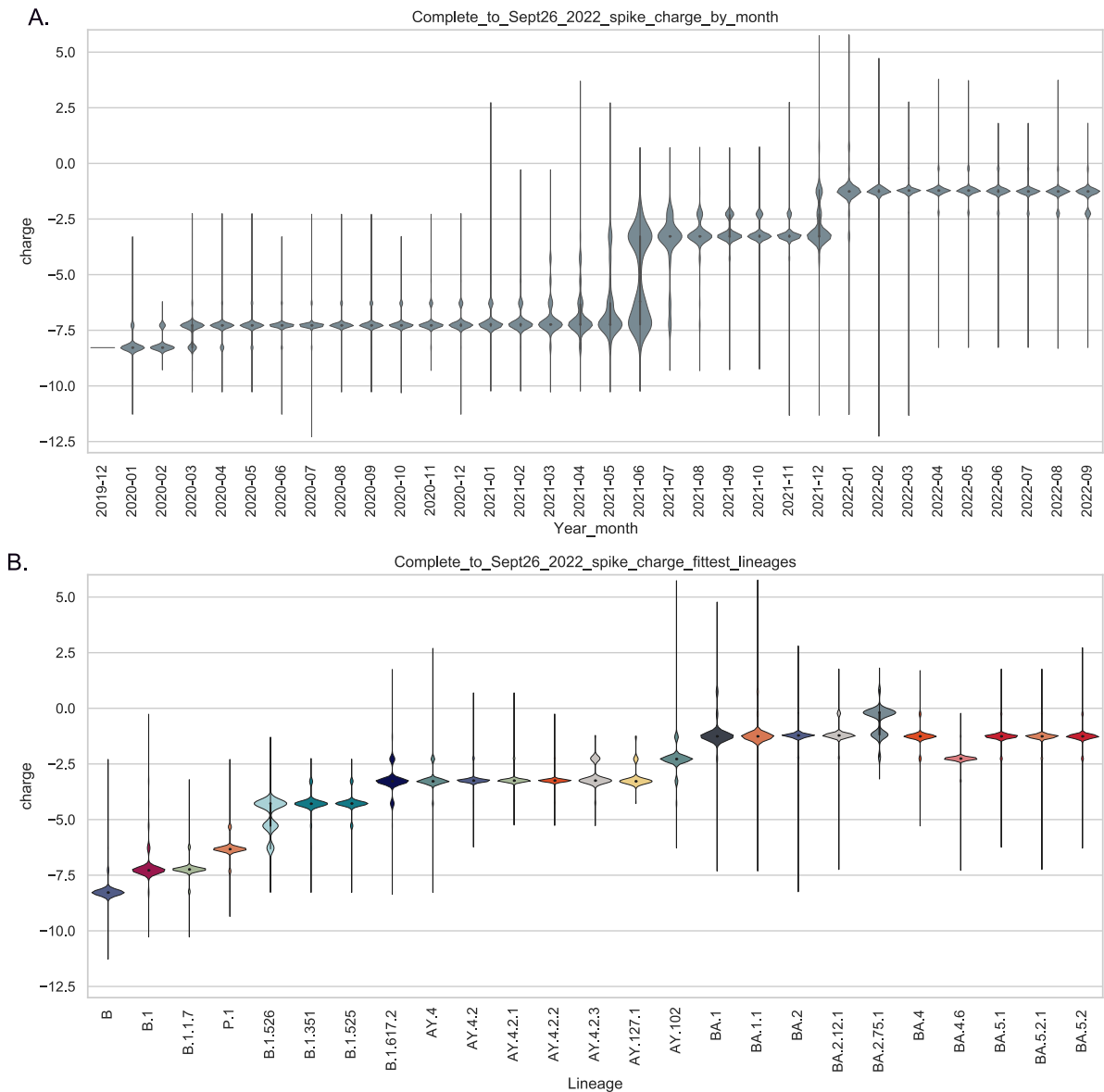
75 which are likely to provide temporary or long-term advantage for the viral lineage. An analysis was  
76 performed to identify spike physical features most strongly linked with SARS-CoV-2 lineages (Figure  
77 1). The first 300 reported genomes from each major lineage were collected, spike protein sequences  
78 were extracted and the physical features of each protein were collected into a matrix. The top features  
79 distinguishing SARS-CoV-2 lineages were identified with charge as the most important feature (Figure  
80 1A). A principal component analysis using the top 8 features (charge, gravity, fraction T, fraction R,  
81 instability, fraction G, fraction D and fraction K), provided clustering of spike sequences by lineage  
82 (Figure 1B). These results support the idea that spike protein charge (among other features) is an  
83 important determinant of the lineages that have evolved during the first two years of the COVID-19  
84 epidemic.



85 **Figure 1. Identification of spike protein charge association with SARS-CoV-2 lineage. Panel A:**  
86 A set of 300 spikes sequences extracted from the first 300 SARS-CoV-2 genomes per lineage (by  
87 date of collection) was analyzed, features for each sequence were collected (see Methods). SKLearn  
88 feature selection (Pedregosa, F. and Varoquaux, G. and Gramfort, A. and Michel, V. et al. 2011) was  
89 used to identify features that most accurately identified the sequence lineage. The importance of  
90 features were ranked in order. **Panel B:** The top 8 features (charge, gravity, fraction T, fraction R,  
91 instability, fraction G, fraction D, fraction K) were further used in a principal component analysis to  
92 cluster the same set of SARS-CoV-2 spike sequences. Each node represents a single spike  
93 sequence, nodes were coloured by Pangolin lineage assigned to the genome from which the spike  
94 sequence was obtained. Lineage colouring is explained in the figure legend to the right.

96  
97  
98 Changes in charge of spike protein across the epidemic were investigated. Plotting total spike  
99 charge for all genomes per month of the epidemic showed a clear pattern of increase in charge over  
100 two years of evolution (Figure 2, panel A). Median spike charge was -8.3 in the original SARS-CoV-2

101 viruses reported in late 2019 to early 2020, by March 2020, an increase in positive charge to -7.28  
102 was observed. Subsequently, an additional increase in positive charge occurred in mid-2021 to -3.28,  
103 and most recently a charge increase occurred in late 2020/early 2021 to -1.26.  
104



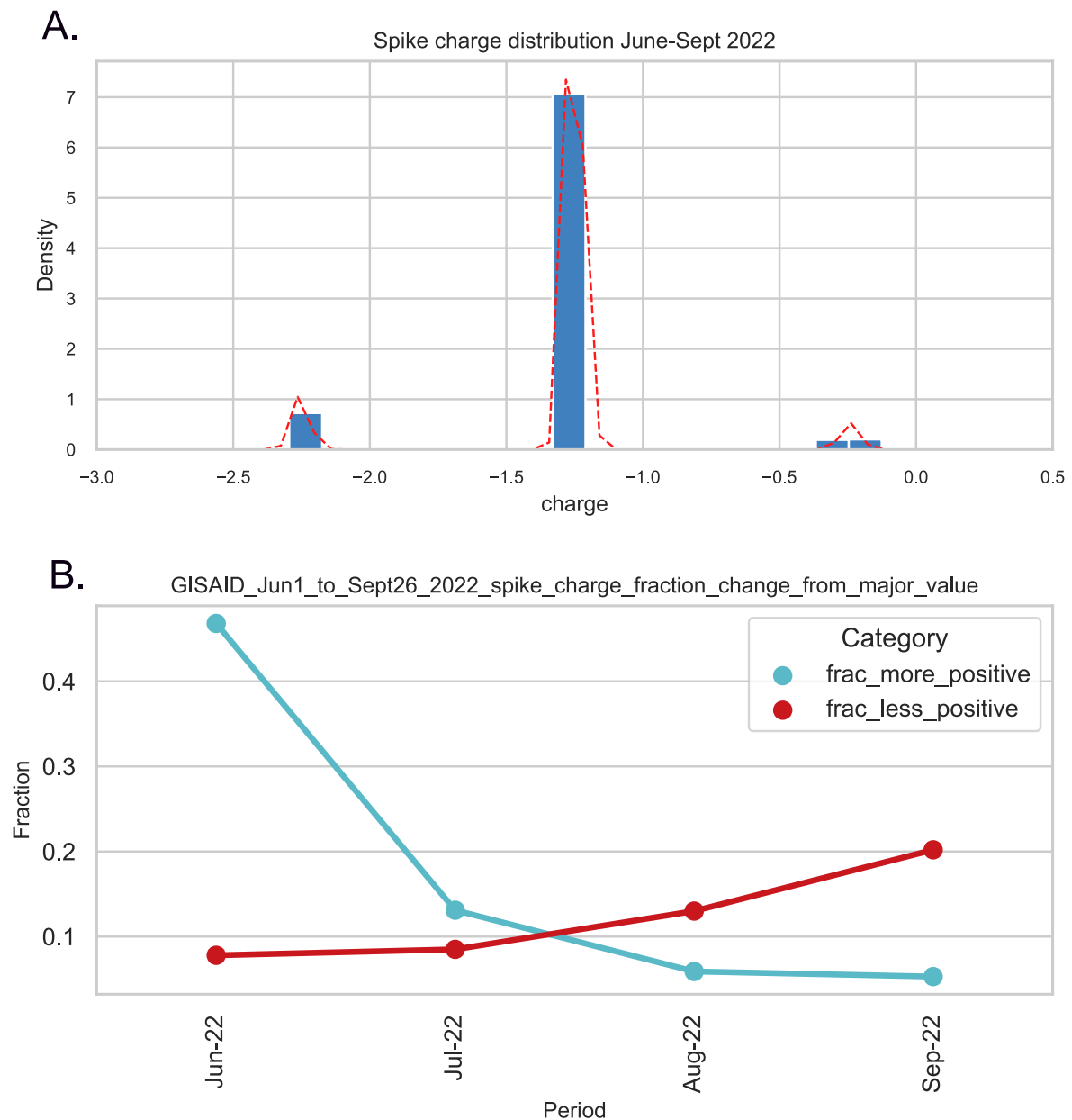
105  
106 **Figure 2. Panel A. Total SARS-CoV-2 spike charge per epidemic month.** All available SARS-CoV-  
107 2 genomes up to 24 September 2022 were retrieved from GISAID (GISAID 2020) and the spike  
108 protein sequence was extracted (if intact). Total charge at pH 7.4 was calculated and values were  
109 plotted using a violin plot by month of sample collection. For each epidemic month the violin plot  
110 depicts the distributions of calculated spike charge for all available SARS-CoV-2 genomes. **Panel B.**  
111 **Spike charge in major SARS-CoV-2 lineages.** For each lineage, all available spike sequences were  
112 collected (up to 24 September 2022), total charge was measured and violin plots prepared to show  
113 the charge distribution by lineage. Lineages (indicated at bottom of chart) were ordered by their  
114 appearance in the epidemic.

115  
116       These spike protein charge increases can be attributed to the major successful lineages  
117 reported over time (Figure 2B). The B.1, B.1.1 and B.1.1.7 (Alpha) lineages that dominated the first  
118 year of the epidemic encoded spike proteins with charges between -8 and -6 while the B.1.351 (Beta)  
119 and B.1.525 (Eta) lineages showed a further increase in charge to around -4.5. The B.1.617.2 (Delta)  
120 lineage and sublineages (AY.x) displayed further increase in charge. Most recently, the Omicron  
121 variants (including BA.1, BA.1.1, BA.2, BA.2.12, BA.3, BA.4 and BA.5) show further spike charge  
122 increases with the majority of Omicron encoded spike proteins showing charge at -1.26 (Figure 2,  
123 panel B).

124       Some indication of functional consequences of the observed changes in spike charge can be  
125 obtained from the location on the charged amino acid substitutions in the spike protein. Sets of spike  
126 sequences (extracted from the first 300 reported genomes per select lineage) were processed to  
127 illustrate the changes to more negative charge (blue) or more positive charge (orange/red) in the  
128 protein relative to the initial Lineage B genome sequences (Supplementary Figure 1). The initial  
129 change in charge was a substitution of an aspartic acid residue (D, with a calculated charge of -1) by  
130 a glycine (G, neutral). In some early lineages (e.g. A.23.1), proline (P) at position 681 was substituted  
131 with the positively charged arginine (R), or Q680 was substituted with a partially charged histidine H  
132 residue. The P681R positive substitution promotes furin cleavage and activation of the spike protein  
133 for cell fusion (Lubinski et al. 2022)(Liu et al. 2022). The Delta lineage spike proteins encoded  
134 additional positive charge in the ACE2 binding region, as well as in the far amino terminal region and  
135 near the heptad repeat (HR1) which may also enhance membrane fusion activity. More recently, a  
136 number of positive substitutions have occurred in the Omicron lineage virus spike proteins with  
137 predominance of positively charged changes in the receptor binding domain (Supplementary Figure  
138 1), suggesting a role of increased charge in spike/receptor interactions.

139       It is probable that the spike protein has an upper limit to the amino acid charge that it can  
140 allow for proper folding, assembly and function. This upper charge value will be determined by the  
141 acquisition of optimum transmission properties in balance with immune selection. After the regular  
142 increase of spike protein charge observed up to the appearance of the Omicron lineages, an  
143 indication of a stasis in positively-charged amino acid accumulation is now displayed by SARS-CoV-2  
144 Omicron lineages. The majority of Omicron sub-lineages remain at spike charge -1.26 (Figure 3A)  
145 although a few specific Omicron sub-lineages show changes toward more positive or negative charge  
146 (e.g. BA.2.75.1 more positive, BA.4.6 more negative, as illustrated in Figure 2B) with the additional  
147 changes often associated with immune selection. To monitor the current trends of spike protein  
148 changes, we calculated the fraction of reported genomes with spike charge greater than or less than  
149 the Omicron mean charge of -1.26 and documented how these fractions had changed over the last 4  
150 months of the pandemic (Figure 3B). The majority of encoded spike proteins are almost exclusively  
151 from Omicron lineage viruses and show a charge of -1.26. However, a small fraction of genomes

152 encode spike proteins with slightly more or less charge (Figure 3B) with the greater trend (20% of all  
153 reported genomes in September 2022) showing more negative charge (Figure 3B).  
154



155  
156 Figure 3. Recent changes in spike protein charge. **Panel A:** All available spike proteins from genomes  
157 with sample collection dates of June-Sept 2022 were analyzed for total spike charge. A histogram of  
158 the calculate total spike charges for the entire set is shown in panel A with the **kernel density**  
159 **estimation (KDE)** line in red. A major peak at -1.26 is observed wit small outlier peaks of genomes  
160 with more negative and more positive spike proteins **Panel B:** For each month (over the period June 1  
161 to Sept 26 2022) the fraction of reported genomes for that month with charge greater than or less than  
162 the majority value of -1.26 was calculated.

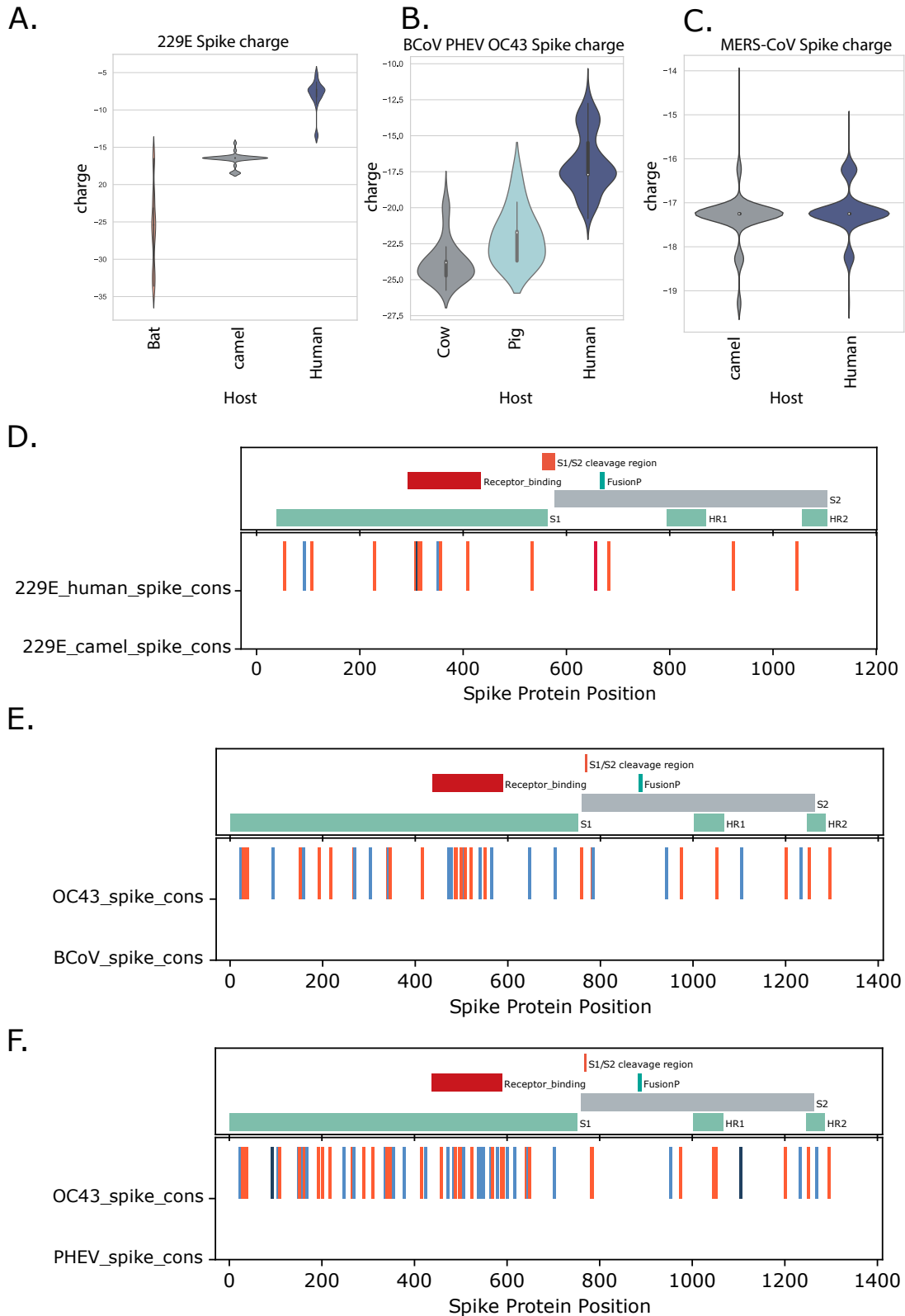
163           Lastly, we investigated if a similar pattern of spike charge evolution could be observed in  
164 other coronaviruses that have made a transition to human transmission. In recent history, several  
165 coronaviruses (in addition to SARS-CoV-2) have been observed to jump hosts. For example,  
166 coronavirus 229E is commonly detected in humans and very close coronaviruses have been identified  
167 in bats (Victor Max Corman et al. 2015) (Tao et al. 2017) and camels (Victor M. Corman et al. 2016)  
168 (Sabir et al. 2016) suggesting movement of the virus between hosts. All available coronavirus 229E  
169 full genomes sequences were retrieved from GenBank, the spike coding region was extracted from  
170 the genomes, translated and total charge was calculated. A difference from -26 to -8, or almost 18  
171 charge units is seen comparing 229E-like viruses from bats to 229E from humans (Figure 4A) and  
172 almost 9 charge unit difference was observed in spike median charge comparing 229E viruses from  
173 camel vs. human infections (Figure 4A).

174           Infection with coronavirus OC43 is common in humans and closely related viruses are found  
175 in cattle (bovine coronavirus, BCoV) (Vijgen et al. 2006) and pigs (porcine hemagglutinating  
176 encephalomyelitis virus, PHEV) (Vijgen et al. 2005) (Vijgen et al. 2006). Comparing the three OC43-  
177 type virus groups, the human virus OC43 has an increased charge of ca. 5 units compared to PHEV  
178 and ca.7 units compared to BCoV (Figure 4B).

179           The commonly known host for the Middle East Respiratory Syndrome coronavirus (MERS-  
180 CoV) is dromedary camels; however, zoonosis and serious human infections occur frequently  
181 (Cotten et al. 2013) (Cotten et al. 2014) (Memish et al. 2014) (Zhou et al. 2021) (So et al. 2019) as  
182 reviewed in (Peiris & Perlman 2022). From 698 full MERS-CoV genomes available in GenBank, there  
183 was no strong difference in the encoded spike charge of virus sequences derived from human versus  
184 camels infections (Figure 4C).

185           Considering the location of the charge differences in the spike proteins, for coronavirus 229E,  
186 the charge increases occurred throughout the protein, although there is a slightly higher number of  
187 positive changes in the receptor binding region of the human infection derived viruses (Figure 4D).  
188 For OC43, the porcine and human viruses also show increases in positive charge throughout the  
189 spike protein, the porcine PHEV also showed a slight enrichment in positive charge in the receptor  
190 binding region (Figure 4E).

191



192  
193  
194  
195

**Figure 4. Spike charges from select groups of coronaviruses that have moved into humans (Panels A-C).** All available full genomes for the indicated coronaviruses were retrieved from



196 GenBank, the spike coding region was identified and translated into protein and total charge at pH 7.4  
197 was calculated. Violin plots indicate the charges of each collection of spike proteins, median values  
198 are indicated by the open square. **Panel A.** Coronavirus 229E from bat, camel or human infections,  
199 **Panel B.** BCoV (from bovine infections) PHEV (from porcine infections) and OC43 (from human  
200 infection), **Panel C.** MERS-CoV from camel or human infection. **Panel D-F: Consensus spike**  
201 **protein sequences were generated from the indicated virus groups and charged amino acid**  
202 **changes were determined.** Charge changes were colored from dark blue (change from positively to  
203 negatively charged amino acid (AA)), blue change from neutral to negatively charged AA), orange  
204 (change from neutral to positively charged AA) and red (change from negative to positively charged  
205 AA). **Panel D:** 229E spike from human infections compared to 229E spike from camel infections,  
206 **Panel E:** Human OC43 spike compared to BCoV spike, **Panel F:** Human OC43 spike compared to  
207 PHEV spike. Key spike protein features of each group's spike protein are shown in the upper portion  
208 of each panel.

209

## 210 Discussion

211 After more than two years of the COVID-19 pandemic and with the availability of >11 million  
212 SARS-CoV-2 genome sequences, a trend of SARS-CoV-2 spike protein charge can be observed,  
213 with successive lineages showing an increase in positive charge over earlier lineages. Over the  
214 course of the pandemic, the SARS-CoV-2 spike protein has evolved from a protein with a total charge  
215 of -8.28 in the original Lineage A and B viruses to a protein with a total charge of -1.26 in the majority  
216 of the currently circulating Omicron lineage viruses. This pattern has been noted previously  
217 (Pawłowski 2021) (Nie et al. 2022). We expand on these observations, and document lineage  
218 patterns and sites of change in the spike protein and explore similar phenomena of evolution to more  
219 positive charge in two other coronaviruses (OC43 and 229E) that have moved between animals and  
220 humans.

221 This study does not identify a mechanistic basis for the increased spike charge although there  
222 are several possible transmission steps that might be promoted by increasing charge. Exposed,  
223 positively charged spike amino acids should promote interactions with negatively charged cellular  
224 structures. Interactions with negatively-charged heparin have been reported with SARS-CoV-2 spike  
225 (Kim et al. 2020) and negatively-charged sialylated glycans are reported to promote entry of SARS-  
226 CoV-2 (Nguyen et al. 2022). The upper respiratory tract is coated by and protected by mucins,  
227 frequently modified with sialic acid or phosphorylated, high mannose N-glycans (Byrd-Leotis et al.  
228 2021) which present a negatively charged matrix that could either promote or protect against viral  
229 transmission. The SARS-CoV-2, OC43, and BCoV virions display binding to negatively charged  
230 carbohydrate structures found in the airway (Byrd-Leotis et al. 2021) and the ionic environment of the  
231 human upper respiratory tract may favour binding and transmission of viruses with increased positive  
232 charge. Perhaps it is not surprising that both OC43 and 229E coronaviruses exhibited increases in  
233 spike positive charge after moving from animal hosts (cow, pig and camel) to human hosts (Figure 5).

234 A similar change in MERS-CoV was not observed, however MERS-CoV currently shows only limited  
235 human to human transmission with most known transmission chains ending after 2 to 3 human to  
236 human transmission events as shown in (Assiri et al. 2013) and (Cotten et al. 2013). MERS-CoV  
237 might not have experienced sufficient number of human replication cycles or have undergone the  
238 same level of selection for human transmission that OC43, 229E and SARS-CoV-2 have experienced.  
239 For both OC43 and 229E coronaviruses moving to humans, the broad location of the positive  
240 changes across the spike protein sequence suggested that positive charge may be promoting several  
241 functions including receptor binding, furin cleavage, cell fusion as well as antigenic changes or less  
242 specific changes to avoid or promote ionic interactions during transmission.

243 There is likely a limit to the accumulation of positively charged residues in the SARS-CoV-2  
244 spike protein. Functional constraints exist, there may also be penalties associated with non-specific  
245 binding due to excess positive charge, and there are certainly charge influences on protein folding  
246 and higher order protein interactions (Creighton 2002). Our prediction is that the SARS-CoV-2 protein  
247 will reach some upper limit of charge defined by these constraints. Indeed, we observe that the  
248 majority of Omicron lineages encode spike proteins with charge -1.26, after more than 6 months of  
249 evolution (Figures 2A and 2B). A small fraction of genomes with more positive charge or less positive  
250 charge have appeared, but the global tendency across all reported genomes from June to September  
251 2022 is a modest decline in the positive charge (Figure 3b) which suggest the upper limit to charge  
252 has been reached.

253 Could these changes in spike charge have occurred by chance and not be a response to  
254 selective pressure? Of the 20 standard amino acids (AA), only 2 AA have negatively charged side  
255 chains, 2 AA have positively charged side chains while the remaining 16 AA are neutral at pH 7.4..  
256 Assuming equal probability of any AA change, there is an 18/20 chance of a negative AA being  
257 substituted by a neutral or positively charged AA and the majority of change opportunities would result  
258 in loss of negative charge. However, natural selection is more complex, because the genetic code  
259 uses 3 adjacent nucleotides to encode an AA, there are multiple encoding possibilities for each AA,  
260 the codon redundancy is not identical for each AA and the number of nucleotide changes required to  
261 produce any particular AA change can be 1, 2 or 3. This has resulted in an evolved protein stability in  
262 the genetic code (Chan et al. 2020) with AA changes that maintain rather than change physical  
263 properties (negative, positive, polar, non-polar, aromatic) more likely based on the codon array  
264 (Livingstone & Barton 1993) and the nucleotide changes required for an AA change. For example, the  
265 probability of a negative AA to negative AA change is 0.333 while the probabilities of change of a  
266 negative AA to a non-polar, aromatic, polar or positive AA are 0.051, 0.044, 0.028 and 0.044  
267 respectively, with changes away from a negative charged AA nearly 10-fold less likely to occur than  
268 conserving the negative charge at that position (Livingstone & Barton 1993). For these reasons, it  
269 appears that the accumulation of positive charge on spike protein has not occurred by chance and is  
270 likely providing some selective advantage for the virus. It should also be noted that the observed  
271 charge changes in exposed virion proteins seem to be limited to spike. Two additional SARS-CoV-2

272 proteins are externally exposed, the E protein (ORF4) and the M protein (ORF5), showing no  
273 consistent change in the charge of either of these proteins across the 2 years of the epidemic (results  
274 not shown).

275 Obermeyer et al. documented AA substitutions associated with SARS-CoV-2 fitness  
276 (Obermeyer et al. 2022). Consistent with the idea that the increase in positive charges is not by  
277 chance, of the top 20 substitutions increasing SARS-CoV-2 fitness, 14 substitutions were in the spike  
278 protein, among which 4 were changes that increased positive charge while only 1 of 14 introduced a  
279 negative charge in spike (Obermeyer et al. 2022).

280 Natural selection could be acting on multiple features of the spike protein. The necessity to  
281 avoid host immune responses is likely to be the major selective force acting on the virus. This results  
282 in the amino acid changes, which in turn are determined by epitopes. The selection for increased  
283 charge in the spike protein is probably occurring in the background, not as a major shift needed to  
284 bypass immune responses. However, the increase in charge may improve survival and transmission  
285 in humans in subtle ways, and this advantage, when multiplied over the millions of infections can  
286 provide some of the growth and infection advantages seen by new SARS-CoV-2 variants. It is  
287 proposed that the N764K, N856K and N969K substitutions (all increasing spike positive charge) may  
288 enhance S1/S2 subunit interactions after proteolytic processing of the spike protein, resulting in  
289 reduced S1 shedding and improving transmission (Martin et al. 2022) Increased charge may also alter  
290 receptor interactions. In the Omicron (BA.1) spike protein, the Q493R and Q498R substitutions are  
291 predicted to allow two additional salt bridges with ACE2 receptor position 35Glu and 38Glu (McCallum  
292 et al. 2022). Indeed, looking at the timing of charge shifts in each major lineage, the changes to more  
293 positive charge accumulate later than the changes that first allow a lineage to emerge and dominate  
294 global infections. In this model, the primary spike changes are driven by immune selection and allow a  
295 new lineage to bypass existing immune responses. Once a successful new variant emerges, the large  
296 number of new infections allow selection for the accumulation of beneficial positive charge changes.  
297 The similar pattern of increased positivity of spike protein in other coronaviruses that have moved  
298 between animals and humans (OC43, 229E, Figure 4) suggest that the change in surface protein  
299 charge may be a more general phenomenon with coronaviruses and might be a useful parameter to  
300 examine when monitoring zoonosis. This study provides a framework to monitor viral evolution  
301 through changes in biochemical properties, which can be easily applied to other viruses important to  
302 public and global health. An important note, our analyses on viral spike protein biochemical properties  
303 to monitor virus evolution are not meant to replace traditional phylogenetic analyses. The observed  
304 pattern of biochemical properties changes should complement phylogenetic signals. However, in  
305 situations where there are limited sequences available to produce reliable phylogenetic signals (e.g.  
306 the 229E and OC43 viruses examined in Figure 4), this kind of analysis using virus biochemical  
307 properties from different host species would certainly help provide important information on the virus  
308 evolution, zoonosis as well as aiding the prediction of patterns of viral changes.

309 In conclusion, our study provides an novel analytical framework to monitor viral evolution  
310 through changes in biochemical properties, which can be easily applied to other viruses important to  
311 public and global health. We also showed that natural virus evolution is more complicated and may  
312 involve multiple factors including immune selection, as well as spike protein biochemical properties.  
313 The observation of increase of SARS-CoV-2 spike protein charge over time provides useful  
314 information for future vaccine and therapeutic development.

315

## 316 **Methods**

317 Full alignments of SARS-CoV-2 genomes were obtained from GISAID (GISAID 2020) with  
318 collection dates to 15 June 2022. All spaces in fasta IDs were removed using sed (sed -i -e 's/ /\_g'  
319 msa\_xxxx.fasta), the alignment was dealigned ("- " characters removed) and genomes were classified  
320 using Pangolin (Áine O'Toole et al. 2020) with the most recent database updates (pangolin v4.1.1,  
321 pangolin-data v1.11  
322 constellations v0.1.10 and scorpio v0.3.17). The spike coding region from each genome (if present  
323 and intact (no Ns)) was translated into protein. Features of the protein that could be quantitated from  
324 the spike protein sequence were determined using the ProteinAnalysis functions from BioPython  
325 (Cock et al. 2009). These features included charge at pH 7.4, Kyle and Doolittle GRAVY score  
326 (Kyte & Doolittle 1982) (a measure of hydrophobicity), an instability index derived from dipeptide  
327 content (Guruprasad et al. 1990), the total percent helix, fold or sheet properties of the protein and the  
328 total fractions of individual amino acids and fractions of di-amino acids. A matrix of all spike protein  
329 features plus collection date, and lineage was prepared and used for analysis. Similar analyses were  
330 performed for other coronaviruses such as 229E, OC43 and MERS-CoV by retrieving all complete  
331 genomes available from GenBank (15 June 2022). The spike protein was also extracted using the  
332 same method as aforementioned. Additional details are provided in the figure legends. The python  
333 code used for the analyses is available here: [https://github.com/mlcotten13/SARS-CoV-](https://github.com/mlcotten13/SARS-CoV-2_spike_charge)  
334 [2\\_spike\\_charge](https://github.com/mlcotten13/SARS-CoV-2_spike_charge) .

335

## 336 **Acknowledgements**

337 We thank all global SARS-CoV-2 sequencing groups for the open sharing of sequence data  
338 and to the GISAID platform and team for making these data available. We are grateful to Andrew  
339 Rambaut, Áine O'Toole and the Pangolin team for the Pangolin typing tool and resources.

340

## 341 **Funding**

342 This work was supported by the UK Medical Research Council (MRC/UK Research and  
343 Innovation) and the UK Department for International Development (DFID) under the MRC/DFID  
344 Concordat agreement (grant agreement no. MC\_PC\_20010) and Wellcome Trust, UK FCDO-  
345 Wellcome Epidemic Preparedness-Coronavirus (grant agreement no. 220977/Z/20/Z).

346

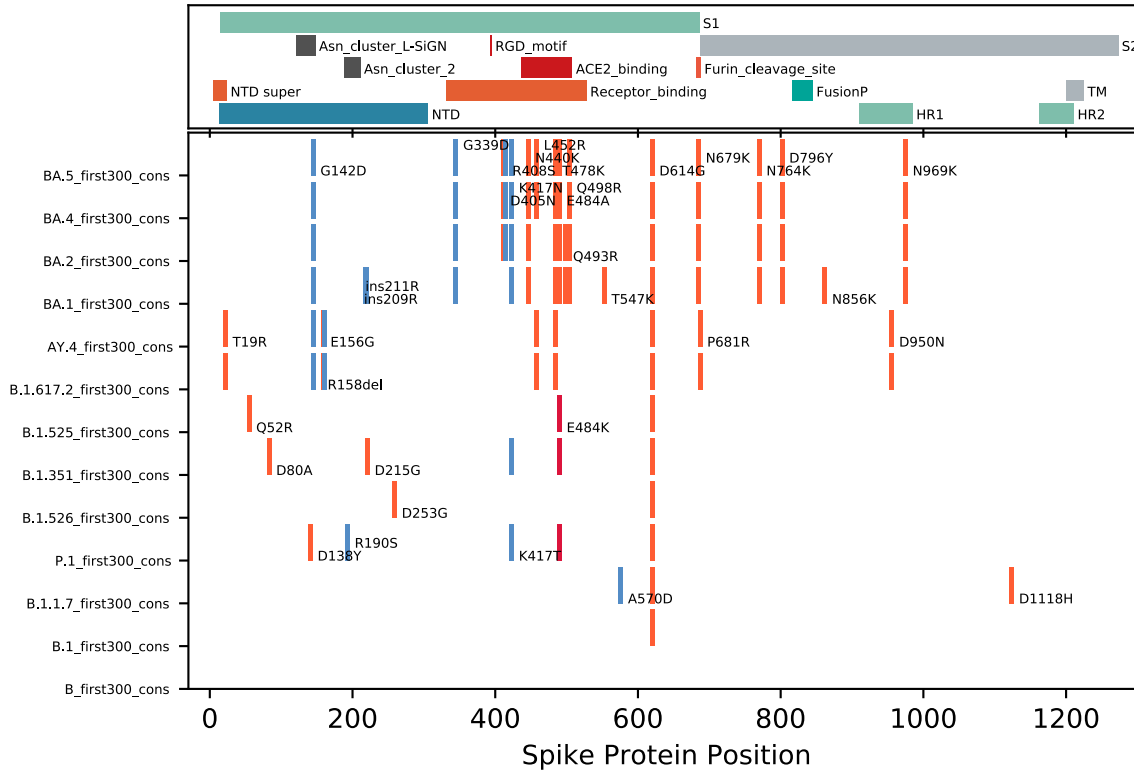
347 **References**

- 348 Adamczyk, Z., Batys, P., & Barbasz, J. (2021). 'SARS-CoV-2 virion physicochemical characteristics  
349 pertinent to abiotic substrate attachment', *Current Opinion in Colloid & Interface Science*, 55:  
350 101466. DOI: 10.1016/j.cocis.2021.101466
- 351 Áine O'Toole et al. (2020). 'Phylogenetic Assignment of Named Global Outbreak LINEages  
352 (PANGOLIN)',.
- 353 Assiri, A., McGeer, A., Perl, T. M., Price, C. S., Al Rabeeah, A. A., Cummings, D. A. T., Alabdullatif, Z.  
354 N., et al. (2013). 'Hospital Outbreak of Middle East Respiratory Syndrome Coronavirus', *New  
355 England Journal of Medicine*, 369/5: 407–16. DOI: 10.1056/NEJMoa1306742
- 356 Byrd-Leotis, L., Lasanajak, Y., Bowen, T., Baker, K., Song, X., Suthar, M. S., Cummings, R. D., et al.  
357 (2021). 'SARS-CoV-2 and other coronaviruses bind to phosphorylated glycans from the  
358 human lung', *Virology*, 562: 142–8. DOI: 10.1016/j.virol.2021.07.012
- 359 Cao, Y., Wang, J., Jian, F., Xiao, T., Song, W., Yisimayi, A., Huang, W., et al. (2022). 'Omicron  
360 escapes the majority of existing SARS-CoV-2 neutralizing antibodies', *Nature*, 602/7898:  
361 657–63. DOI: 10.1038/s41586-021-04385-3
- 362 Chan, K.-F., Koukouravas, S., Yeo, J. Y., Koh, D. W.-S., & Gan, S. K.-E. (2020). 'Probability of  
363 change in life: Amino acid changes in single nucleotide substitutions', *Biosystems*, 193–194:  
364 104135. DOI: 10.1016/j.biosystems.2020.104135
- 365 Cock, P. J. A., Antao, T., Chang, J. T., Chapman, B. A., Cox, C. J., Dalke, A., Friedberg, I., et al.  
366 (2009). 'Biopython: freely available Python tools for computational molecular biology and  
367 bioinformatics', *Bioinformatics*, 25/11: 1422–3. DOI: 10.1093/bioinformatics/btp163
- 368 Corman, Victor M., Eckerle, I., Memish, Z. A., Liljander, A. M., Dijkman, R., Jonsdottir, H., Juma  
369 Ngeiywa, K. J. Z., et al. (2016). 'Link of a ubiquitous human coronavirus to dromedary  
370 camels', *Proceedings of the National Academy of Sciences*, 113/35: 9864–9. DOI:  
371 10.1073/pnas.1604472113
- 372 Corman, Victor Max, Baldwin, H. J., Tateno, A. F., Zerbinati, R. M., Annan, A., Owusu, M., Nkrumah,  
373 E. E., et al. (2015). 'Evidence for an Ancestral Association of Human Coronavirus 229E with  
374 Bats', (S. Schultz-Cherry, Ed.) *Journal of Virology*, 89/23: 11858–70. DOI: 10.1128/JVI.01755-  
375 15
- 376 Cotten, M., Watson, S. J., Kellam, P., Al-Rabeeah, A. A., Makhdoom, H. Q., Assiri, A., Al-Tawfiq, J.  
377 A., et al. (2013). 'Transmission and evolution of the Middle East respiratory syndrome  
378 coronavirus in Saudi Arabia: a descriptive genomic study', *Lancet (London, England)*,  
379 382/9909: 1993–2002. DOI: 10.1016/S0140-6736(13)61887-5
- 380 Cotten, M., Watson, S. J., Zumla, A. I., Makhdoom, H. Q., Palser, A. L., Ong, S. H., Al Rabeeah, A.  
381 A., et al. (2014). 'Spread, circulation, and evolution of the Middle East respiratory syndrome  
382 coronavirus', *mBio*, 5/1: e01062-13. DOI: 10.1128/mBio.01062-13
- 383 Creighton, T. E. (2002). *Proteins: structures and molecular properties.*, 2. ed., [Nachdr.]. New York:  
384 Freeman.
- 385 DeGrace, M. M., Ghedin, E., Frieman, M. B., Krammer, F., Grifoni, A., Alisoltani, A., Alter, G., et al.  
386 (2022). 'Defining the risk of SARS-CoV-2 variants on immune protection', *Nature*, 605/7911:  
387 640–52. DOI: 10.1038/s41586-022-04690-5
- 388 Dejnirattisai, W., Huo, J., Zhou, D., Zahradník, J., Supasa, P., Liu, C., Duyvesteyn, H. M. E., et al.  
389 (2022). 'SARS-CoV-2 Omicron-B.1.1.529 leads to widespread escape from neutralizing  
390 antibody responses', *Cell*, 185/3: 467-484.e15. DOI: 10.1016/j.cell.2021.12.046
- 391 GISAID. (2020). 'The GISAID Initiative',.
- 392 Greaney, A. J., Loes, A. N., Crawford, K. H. D., Starr, T. N., Malone, K. D., Chu, H. Y., & Bloom, J. D.  
393 (2021). 'Comprehensive mapping of mutations in the SARS-CoV-2 receptor-binding domain  
394 that affect recognition by polyclonal human plasma antibodies', *Cell Host & Microbe*, 29/3:  
395 463-476.e6. DOI: 10.1016/j.chom.2021.02.003
- 396 Greaney, A. J., Starr, T. N., Barnes, C. O., Weisblum, Y., Schmidt, F., Caskey, M., Gaebler, C., et al.  
397 (2021). 'Mapping mutations to the SARS-CoV-2 RBD that escape binding by different classes  
398 of antibodies', *Nature Communications*, 12/1: 4196. DOI: 10.1038/s41467-021-24435-8

- 399 Greaney, A. J., Starr, T. N., & Bloom, J. D. (2022). 'An antibody-escape estimator for mutations to the  
400 SARS-CoV-2 receptor-binding domain', *Virus Evolution*, 8/1: veac021. DOI:  
401 10.1093/ve/veac021
- 402 Guruprasad, K., Reddy, B. V. B., & Pandit, M. W. (1990). 'Correlation between stability of a protein  
403 and its dipeptide composition: a novel approach for predicting *in vivo* stability of a protein from  
404 its primary sequence', *Protein Engineering, Design and Selection*, 4/2: 155–61. DOI:  
405 10.1093/protein/4.2.155
- 406 Kim, S. Y., Jin, W., Sood, A., Montgomery, D. W., Grant, O. C., Fuster, M. M., Fu, L., et al. (2020).  
407 'Characterization of heparin and severe acute respiratory syndrome-related coronavirus 2  
408 (SARS-CoV-2) spike glycoprotein binding interactions', *Antiviral Research*, 181: 104873. DOI:  
409 10.1016/j.antiviral.2020.104873
- 410 Kyte, J., & Doolittle, R. F. (1982). 'A simple method for displaying the hydropathic character of a  
411 protein', *Journal of Molecular Biology*, 157/1: 105–32. DOI: 10.1016/0022-2836(82)90515-0
- 412 Liu, Y., Liu, J., Johnson, B. A., Xia, H., Ku, Z., Schindewolf, C., Widen, S. G., et al. (2022). 'Delta  
413 spike P681R mutation enhances SARS-CoV-2 fitness over Alpha variant', *Cell Reports*, 39/7:  
414 110829. DOI: 10.1016/j.celrep.2022.110829
- 415 Livingstone, C. D., & Barton, G. J. (1993). 'Protein sequence alignments: a strategy for the  
416 hierarchical analysis of residue conservation', *Bioinformatics*, 9/6: 745–56. DOI:  
417 10.1093/bioinformatics/9.6.745
- 418 Lubinski, B., Frazier, L. E., Phan, M. V. T., Bugembe, D. L., Cunningham, J. L., Tang, T., Daniel, S.,  
419 et al. (2022). 'Spike Protein Cleavage-Activation in the Context of the SARS-CoV-2 P681R  
420 Mutation: an Analysis from Its First Appearance in Lineage A.23.1 Identified in Uganda',  
421 *Microbiology Spectrum*, e0151422. DOI: 10.1128/spectrum.01514-22
- 422 Martin, D. P., Lytras, S., Lucaci, A. G., Maier, W., Grüning, B., Shank, S. D., Weaver, S., et al. (2022).  
423 'Selection analysis identifies clusters of unusual mutational changes in Omicron lineage BA.1  
424 that likely impact Spike function', (K. Crandall, Ed.) *Molecular Biology and Evolution*, msac061.  
425 DOI: 10.1093/molbev/msac061
- 426 McCallum, M., Czudnochowski, N., Rosen, L. E., Zepeda, S. K., Bowen, J. E., Walls, A. C., Hauser,  
427 K., et al. (2022). 'Structural basis of SARS-CoV-2 Omicron immune evasion and receptor  
428 engagement', *Science*, 375/6583: 864–8. DOI: 10.1126/science.abn8652
- 429 Memish, Z. A., Cotten, M., Meyer, B., Watson, S. J., Alshahfi, A. J., Al Rabeeah, A. A., Corman, V. M.,  
430 et al. (2014). 'Human infection with MERS coronavirus after exposure to infected camels,  
431 Saudi Arabia, 2013', *Emerging Infectious Diseases*, 20/6: 1012–5. DOI:  
432 10.3201/eid2006.140402
- 433 Nguyen, L., McCord, K. A., Bui, D. T., Bouwman, K. M., Kitova, E. N., Elaish, M., Kumawat, D., et al.  
434 (2022). 'Sialic acid-containing glycolipids mediate binding and viral entry of SARS-CoV-2',  
435 *Nature Chemical Biology*, 18/1: 81–90. DOI: 10.1038/s41589-021-00924-1
- 436 Nie, C., Sahoo, A. K., Netz, R. R., Herrmann, A., Ballauff, M., & Haag, R. (2022). 'Charge Matters:  
437 Mutations in Omicron Variant Favor Binding to Cells', *ChemBioChem*. DOI:  
438 10.1002/cbic.202100681
- 439 Obermeyer, F., Jankowiak, M., Barkas, N., Schaffner, S. F., Pyle, J. D., Yurkovetskiy, L., Bosso, M.,  
440 et al. (2022). 'Analysis of 6.4 million SARS-CoV-2 genomes identifies mutations associated  
441 with fitness', *medRxiv: The Preprint Server for Health Sciences*, 2021.09.07.21263228. DOI:  
442 10.1101/2021.09.07.21263228
- 443 Pawłowski, P. (2021). 'SARS-CoV-2 variant Omicron (B.1.1.529) is in a rising trend of mutations  
444 increasing the positive electric charge in crucial regions of spike protein S.', *Acta Biochimica  
445 Polonica*. DOI: 10.18388/abp.2020\_6072
- 446 Pedregosa, F. and Varoquaux, G. and Gramfort, A. and Michel, V., and Thirion, B. and Grisel, O. and  
447 Blondel, M. and Prettenhofer, P., and Weiss, R. and Dubourg, V. and Vanderplas, J. and  
448 Passos, A. and, & Cournapeau, D. and Brucher, M. and Perrot, M. and Duchesnay, E. (2011).  
449 'Scikit-learn: Machine Learning in Python', *Journal of Machine Learning Research*, 12: 2825–  
450 30.
- 451 Peiris, M., & Perlman, S. (2022). 'Unresolved questions in the zoonotic transmission of MERS',  
452 *Current Opinion in Virology*, 52: 258–64. DOI: 10.1016/j.coviro.2021.12.013

- 453 Sabir, J. S. M., Lam, T. T.-Y., Ahmed, M. M. M., Li, L., Shen, Y., E. M. Abo-Aba, S., Qureshi, M. I., et  
454 al. (2016). 'Co-circulation of three camel coronavirus species and recombination of MERS-  
455 CoVs in Saudi Arabia', *Science*, 351/6268: 81–4. DOI: 10.1126/science.aac8608
- 456 So, R. T. Y., Chu, D. K. W., Miguel, E., Perera, R. A. P. M., Oladipo, J. O., Fassi-Fihri, O., Aylet, G., et  
457 al. (2019). 'Diversity of Dromedary Camel Coronavirus HKU23 in African Camels Revealed  
458 Multiple Recombination Events among Closely Related Betacoronaviruses of the Subgenus  
459 Embecovirus', *Journal of Virology*, 93/23: e01236-19. DOI: 10.1128/JVI.01236-19
- 460 Tao, Y., Shi, M., Chommanard, C., Queen, K., Zhang, J., Markotter, W., Kuzmin, I. V., et al. (2017).  
461 'Surveillance of Bat Coronaviruses in Kenya Identifies Relatives of Human Coronaviruses  
462 NL63 and 229E and Their Recombination History', (S. Perlman, Ed.) *Journal of Virology*, 91/5:  
463 e01953-16. DOI: 10.1128/JVI.01953-16
- 464 Tzou, P. L., Tao, K., Pond, S. L. K., & Shafer, R. W. (2022). 'Coronavirus Resistance Database (CoV-  
465 RDB): SARS-CoV-2 susceptibility to monoclonal antibodies, convalescent plasma, and  
466 plasma from vaccinated persons', (J. Bhattacharya, Ed.) *PLOS ONE*, 17/3: e0261045. DOI:  
467 10.1371/journal.pone.0261045
- 468 Vijgen, L., Keyaerts, E., Lemey, P., Maes, P., Van Reeth, K., Nauwynck, H., Pensaert, M., et al.  
469 (2006). 'Evolutionary history of the closely related group 2 coronaviruses: porcine  
470 hemagglutinating encephalomyelitis virus, bovine coronavirus, and human coronavirus  
471 OC43', *Journal of Virology*, 80/14: 7270–4. DOI: 10.1128/JVI.02675-05
- 472 Vijgen, L., Keyaerts, E., Moës, E., Thoelen, I., Wollants, E., Lemey, P., Vandamme, A.-M., et al.  
473 (2005). 'Complete genomic sequence of human coronavirus OC43: molecular clock analysis  
474 suggests a relatively recent zoonotic coronavirus transmission event', *Journal of Virology*,  
475 79/3: 1595–604. DOI: 10.1128/JVI.79.3.1595-1604.2005
- 476 Zhou, Z., Hui, K. P. Y., So, R. T. Y., Lv, H., Perera, R. A. P. M., Chu, D. K. W., Gelaye, E., et al.  
477 (2021). 'Phenotypic and genetic characterization of MERS coronaviruses from Africa to  
478 understand their zoonotic potential', *Proceedings of the National Academy of Sciences of the  
479 United States of America*, 118/25: e2103984118. DOI: 10.1073/pnas.2103984118

481



482

483 **Supplementary Figure 1. Location of charged amino acid changes in the spike protein.** The  
 484 spike protein sequences encoded by the first 300 reported genomes for the indicated SARS-CoV-2  
 485 lineages were collected, and charged amino acid changes from the original B lineage spike sequence  
 486 were plotted. Charge changes were colored from dark blue (change from positive to negative  
 487 charged amino acid (AA)), blue change from neutral to negative charged AA), orange (change from  
 488 neutral to positive charged AA) and red (change from negative to positive charged AA). Substitutions  
 489 are indicated by original AA/position in reference sequence spike/novel AA. The GenBank  
 490 NC\_045512 genome was used as reference. Key spike protein features of the SARS-CoV-2 spike  
 491 protein are shown in the upper panel of the figure.